IEEE Access
Multidisciplinary | Rapid Review | Open Access Journal

Received March 19, 2020, accepted April 28, 2020, date of publication May 8, 2020, date of current version May 28, 2020.

Digital Object Identifier 10.1109/ACCESS.2020.2993279

Research on Modeling and Deep Peak Regulation Control of a Combined Heat and Power Unit

YAOKUI GAO[1], DELIANG ZENG[1], LIXIA ZHANG[2], YONG HU[1], AND ZEKUN XIE[2]
[1]State Key Laboratory of Alternate Electrical Power System with Renewable Energy Sources, North China Electric Power University, Beijing 102206, China
[2]School of Control and Computer Engineering, North China Electric Power University, Beijing 102206, China

Corresponding author: Yaokui Gao (gaoyaokui05@126.com)

This work was supported in part by the National Natural Science Foundation of China under Grant 51776065, and in part by the China Postdoctoral Science Foundation under Grant 2018M641292.

ABSTRACT This paper firstly proposes a nonlinear dynamic model of a combined heat and power (CHP) unit with absorption heat pump (AHP) and bypass systems, the unknown parameters are determined based on design data and perturbation test. Simulation results show that the model can reveal the couplings of AHP and bypass systems to the CHP unit, and provide model support for controller design. On the basis of the model, this paper further proposes a deep peak regulation control strategy, in which, the generalized predictive control algorithm with feedforward-feedback structure is adopted to fundamentally solve the control problems of large delay and inertia on the boiler side, and overcome known disturbances on the turbine side; the ratio of the first stage pressure to the exhaust pressure from high pressure cylinder is adopted to control the high pressure bypass. The deep peak regulation process is divided into two stages: 1) CHP and AHP are used for heating when their heating capacity can meet the heat load requirements of residents, 2) as the unit load is further reduced, bypass mode is activated for heating when the steam flow entering the low pressure cylinder is lower than its cooling flow. Simulation results show that the strategy can meet the heat load requirements of residents and ensure the safe and stable operation of the turbine when the unit is in deep peak regulation condition.

INDEX TERMS Combined heat and power unit, absorption heat pump, bypass heating, dynamic model, deep peak regulation control.

I. INTRODUCTION

In recent years, with the support of policies [1], [2], the installed capacity of wind power has been growing rapidly in China [3], however, the phenomenon of abandoning wind power is serious [4], especially in northeast China [5]. The main reason lies in the scarcity of power supply that can participate in deep peaking, such as hydropower and condensing power [6]. Instead, there are many combined heat and power (CHP) units in these area, but these units need to balance the heat load requirements of residents. In this case, CHP units are prone to excessive power generation when the electrical load demand is low, thus making the space for wind power integration insufficient. Obviously, if the ''ordering power by heat'' constraint of CHP units is decoupled during this periods [7], the power generated by CHP units can be reduced, in this case, huge grid-connected space can be created for wind power. Consequently, decoupling the constraint of CHP units is an important way to solve the problem of wind power consumption in northeast China.

The main methods to decouple the constraint of CHP units are absorption heat pump (AHP) [8], [9], bypass [10], electric boiler) [11]–[13], heat storage tank [14], [15], low pressure cylinder (LPC) removal [16], high back pressure [17], etc. This paper mainly study a CHP unit with AHP and bypass systems. Driven by steam, AHP can recycle the waste heat from the circulating water and heat the return water. Since the low-grade heat source is used for heating, the energy-saving effect of the AHP is remarkable. Bypass supplies heat by reducing the parameters of high-grade heat sources, which will cause certain energy loss. Since the bypass heating mode deviates from the design condition of CHP units, which may increase the component loss and affect the service life of CHP units during long-term operation.

Currently, scholars at home and abroad have done a lot of research on the above two methods, but mainly focuses on efficiency and scheduling. In terms of efficiency, [18] proposed a new waste heat recovery scheme based on AHP,

The associate editor coordinating the review of this manuscript and approving it for publication was Lei Wang.

which provides a theoretical basis for the design of CHP units with AHP. Reference [19], [20] analyzed the heating performance of an AHP, clarified the change and distribution of energy during heating, and proposed a new CHP system. Results show that the new system can improve the efficiency and reduce the energy consumption. In terms of scheduling, [21] proposed a scheduling model for a CHP unit based on heat transfer principle. This model can adapt to the situation that the CHP unit deviates from the design condition. Reference [22] described a tractable integrated heat and electricity dispatch model, this model focuses on the thermal inertia characteristics of pipelines and buildings to increase flexibility.

In summary, the research on modeling and deep peak regulation control of CHP units is insufficient, especially for CHP units equipped with AHP and bypass systems. Therefore, this paper firstly proposes a nonlinear dynamic model of a CHP unit with AHP and bypass systems, gives the method for determining the unknown parameters, and verifies the effectiveness of the model. Based on the model, a deep peak regulation control is proposed based on generalized predictive control algorithm. Simulation results show that the strategy can achieve deep peak regulation of the CHP unit.

The paper is organized as follows. Section 2 introduces the working principle of a CHP unit with AHP and bypass systems, proposes a nonlinear dynamic model of the CHP unit, designs and verifies a deep peak regulation control strategy for the CHP unit. Section 3 elaborates conclusions.

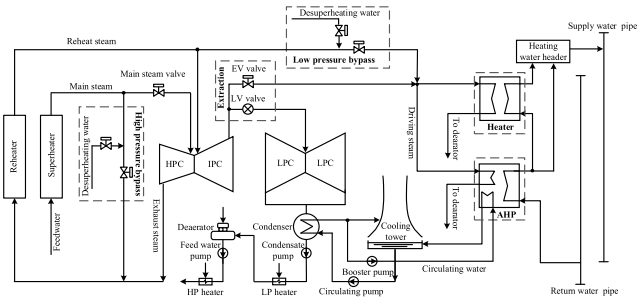

FIGURE 1. **Working principle of a CHP unit with AHP and bypass systems.**

II. MODELING, CONTROL AND ANALYSIS

A. WORKING PPRINCIPLE

As shown in **FIGURE 1**, in addition to the extraction heating mode, the CHP unit has also been improved to some extent. Firstly, a bypass heating system is added. Part of main steam is desuperheated and decompressed by high pressure bypass (HPB), and then mixed with the exhaust steam from the high pressure cylinder (HPC), the mixed steam is sent to the reheater for reheating. After reheating, part of reheat steam is further desuperheated and decompressed by low pressure bypass (LPB) and mixed with the extraction steam from the intermediate pressure cylinder (IPC), this mixed steam is actually prepared for heating. Part of the heating steam is used as the driving steam to enter the AHP, while the other part of the heating steam directly enter the heater for heating. Secondly, an AHP heating system is added. Driven by the steam, the heat consists in circulating water can be recycled by AHP heating system, the recycled heat is then used to heat the return water initially. After the initial heating, the return water is divided into two parts: one part enters the heater to continue absorb heat, thereby further increasing the temperature of return water; the other part directly enters the header for mixing, so that the temperature of the mixed water can meet the heat load requirements of residents.

For bypass system [10], the steam flows into the cold section of the reheater increases with the opening of the HPB valve, since the resistance of the reheater remains unchanged, more steam flows through the reheater, resulting in the differential pressure of the reheater to increase. If the LPB valve is not opened in time, the exhaust steam pressure from HPC will be increased rapidly. Since the temperature and pressure of the steam are coupled, the exhaust steam temperature from HPC will also be increased. Excessive pressure and temperature of exhaust steam will cause changes in the flow characteristics of the HPC, as a result, the balance of the original axial thrust will be broken. In this case, the strength of the final stage blades for the HPC will also be affected. Therefore, it is necessary to open the LPB valve timely to ensure that the exhaust parameters from the HPC is within a reasonable range.

For AHP systems [23], it is necessary to raise the back pressure of CHP units to 7kPa to ensure that the temperature of circulating water can meet the design parameters of AHP systems. Since the increase of the back pressure directly increases the cooling flow of the LPC, the heating capacity of the CHP units transformed by AHP systems will be reduced, especially under low load conditions, the situation that the AHP heating mode and the extraction heating mode cannot be put into operation at the same time may occur. That is: the extraction heating mode may not be able to put into operation when the AHP has been put into operation, which is due to the limitation of the cooling flow for the LPC; the same reason, the back pressure of CHP units may not be able to raise when extraction heating mode is put into operation, as a result, the temperature of circulating water will be insufficient for normal operation of AHP systems.

B. DYNAMIC MODEL

1) MODEL STRUCTURE

Currently, the boiler model is relatively mature [24], [25], but the model with bypass systems has not yet appeared. Therefore, this paper firstly improves the boiler model, the improved model includes a pulverizing system model (Eq.(1)), a drum model (Eq.(2)), and a main steam pipe model (Eq.(3)) and a reheat steam pipe model (Eq.(4) and Eq.(5)).

$$T_f \frac{dq_f}{dt} = -q_f + q_b\,(t-\tau) \tag{1}$$

$$C_b \frac{dp_b}{dt} = K_1 q_f - K_2\sqrt{p_b - p_t} \tag{2}$$

$$C_t \frac{dp_t}{dt} = K_2\sqrt{p_b - p_t} - K_3 p_t u_t - K_4 p_t u_i^{HPB} \quad (3)$$

$$C_r \frac{dp_r}{dt} = D_r - 100K_7 p_r - K_8 p_r u_i^{LPB} \quad (4)$$

$$D_r = K_5 K_3 p_t u_t - K_6 K_4 p_t u_i^{HPB} \quad (5)$$

where q_b is coal feed flow, t/h; q_f is the amount of coal entering the boiler, t/h; τ is the delay time of the coal feeder, s; T_f is the inertia time of the coal mill and the separator, s; C_b is the storage coefficient of steam drum, (t/h·s)/MPa. p_b is the drum pressure, MPa; p_t is main steam pressure, MPa; C_t is the storage coefficient of main steam pipe, (t/h·s)/MPa. u_t is the position of main steam valve, %; u_i^{HPB} is the positon of HPB valve, %; C_r is the storage coefficient of reheat steam pipe, (t/h·s)/MPa; D_r is the reheat steam flow, t/h; p_r is the reheat steam pressure, MPa; u_i^{LPB} is the positon of LPB valve, %; τ, T_f, C_b, C_t, C_r are dynamic parameters that need to be determined, $K_1, \ldots, K_8$ are static parameters that need to be determined.

The ratio of the first stage pressure to the exhaust pressure from HPC is a parameter that needs to be monitored when bypass heating mode is put into operation (Eq.(6)).

$$R^{HPC} = \frac{100u_t p_t}{p_r} \quad (6)$$

The saturation temperature of water in the heater reflects the balance between a) the heat consists in exhaust steam from IPC, the heat consists in the steam generated by the LPB and b) the heat entering the LPC, the heat entering the heater. Thus the saturation temperature of water in the heater is selected as a state variable. Thus, the model of heater is as show in Eq. (7) and Eq.(8).

$$M_h^{HTR}\frac{d\theta_{sw}^{HTR}}{dt} = Q_h^{HTR} - \frac{1}{3600}q_h^{HTR}c_{p,x}(\theta_o^{HTR} - \theta_i^{HTR}) \quad (7)$$

$$\Delta\theta^{HTR} = \theta_{sw}^{HTR} - \theta_o^{HTR} \quad (8)$$

where M_{sw}^{HTR} is the temperature-based storage coefficient of the heater, MJ/°C; θ_{sw}^{HTR} is the saturation temperature of water in the heater, °C; Q_{sw}^{HTR} is the heat released by the steam entering the heater, MJ/s; q_{sw}^{HTR} is the return water flow entering the heater, t/h; $c_{p,x}$ is the specific heat capacity of the return water, MJ/(t·°C); $\Delta\theta^{HTR}$ is the terminal difference of the heater, °C; θ_o^{HTR} is the outlet water temperature of the heater, °C; θ_i^{HTR} is the inlet water temperature of the heater, °C.

Since there is a large inertia and delay in the transmission process of θ_{sw}^{HTR}, θ_{sw}^{HTR} is not suitable to be taken as a state variable. For this reason, [10] fits θ_{sw}^{HTR} as a linear function of p_o^{IPC} (Eq.(9)). Assume that the terminal difference of the heater $\Delta\theta^{HTR} = 10$°C, then the outlet temperature of the heater is as show in Eq.(10).

$$\theta_{sw}^{HTR} = 95.5p_o^{IPC} + 103.38 \quad (9)$$

$$\theta_o^{HTR} = 95.5p_o^{IPC} + 93.38 \quad (10)$$

Substitute Eq. (9) and (10) into Eq. (7), take $c_{p,x} = 4.1882$ MJ/(t·°C), then, the following equation can be obtained:

$$95.5M_h^{HTR}\frac{dp_o^{IPC}}{dt} = Q_h^{HTR} - \frac{4.1882}{3600} \times q_h^{HTR}(95.5p_o^{IPC} - \theta_i^{HTR} + 93.38) \quad (11)$$

Let $C_h^{HTR} = 95.5M_h^{HTR}$, then:

$$C_h^{HTR}\frac{dp_o^{IPC}}{dt} = Q_h^{HTR} - \frac{4.1882}{3600} \times q_h^{HTR}(95.5p_o^{IPC} - \theta_i^{HTR} + 93.38) \quad (12)$$

The heat released by the steam entering the heater Q_h^{HTR} is actually related to the enthalpy of exhaust steam from the IPC, the saturation enthalpy of water in the heater, and the steam flow entering the heater. Therefore, the heat released by the steam entering the heater Q_h^{HTR} can be calculated as:

$$Q_h^{HTR} = \frac{1}{3600}D_h^{HTR}(h_o^{IPC} - h_{sw}^{HTR}) \quad (13)$$

$$D_h^{HTR} = 100K_9K_7p_r + K_{10}K_8p_r u_i^{LPB} - K_{11}p_o^{IPC}u_i^{LPC} - K_{12}p_o^{IPC}u_i^{AHP} \quad (14)$$

where D_h^{HTR} is the steam flow entering the heater, t/h; h_o^{IPC} is the exhaust enthalpy steam from IPC, kJ/kg, $h_o^{IPC} = 2992.85$ kJ/kg; h_{sw}^{HTR} is the saturation enthalpy of water in the heater, kJ/kg, which can be fitted by p_o^{IPC} (Eq.(15)); u_i^{LPC} inlet valve position of LPC, %; u_i^{AHP} is the inlet valve position of AHP, %.

$$h_{sw}^{HTR} = 436.62p_o^{IPC} + 421.03 \quad (15)$$

The coefficient of performance (COP) is a key parameter reflecting the performance of AHP, which can be defined as follows:

$$COP = \frac{Q_1}{W} = \frac{Q_2 + W}{W} \quad (16)$$

where Q_1 is the heat output from AHP, MW; Q_2 is the heat absorbed from circulating water, MW; W is the heat released by driving steam, MW; Q_2 and W can be calculated according to Eq. (17) and (18) respectively.

$$Q_2 = \frac{1}{3600}q_c^{AHP}c_{p,x}(\theta_{ci}^{AHP} - \theta_{co}^{AHP}) \quad (17)$$

$$W = \frac{1}{3600}D_h^{AHP}(h_o^{IPC} - h_{sw}^{AHP}) \quad (18)$$

where q_c^{AHP} is the circulating water flow, t/h; θ_{ci}^{AHP} is the inlet temperature of circulating water, °C; θ_{co}^{AHP} is the outlet temperature of circulating water, °C; D_h^{AHP} is the driving steam flow, t/h; h_{sw}^{AHP} is the saturation enthalpy of water in AHP, kJ/kg. Based on the design parameters of the AHP (**TABLE 2**), Q_2, W and COP can be calculated: $Q_2 = 21.72$MW, $W = 32.035$MW, COP $= 1.68$.

Assume that the COP of the AHP is unchanged during operation, then the heat transfer process of AHP can be

described as show in Eq.(19), in this case, the outlet temperature of heating water can be obtained (Eq.(20)).

$$D_h^{AHP}(h_o^{IPC}-h_{sw}^{IPC})\times COP = q_c^{AHP}c_{p,x}(\theta_{ho}^{AHP}-\theta_{hi}^{AHP}) \tag{19}$$

$$\theta_{ho}^{AHP} = \frac{1.68D_h^{AHP}(h_o^{IPC}-h_{sw}^{IPC})}{q_c^{AHP}c_{p,x}}+\theta_{hi}^{AHP} \tag{20}$$

where θ_{hi}^{AHP} is the inlet temperature of heating water, °C; θ_{ho}^{AHP} is the outlet temperature of heating water, °C.

In actual application, the heating water output from AHP is divided into two parts, one part of the water enter the heater for further heating, while the other part of the water enters the heating water header. These two parts of water are mixed in the header. Ignoring the change in the specific heat capacity of the water, the temperature of the mixed water can be calculated as show in Eq. (21).

$$\theta_{mix} = \frac{q_h^{HTR}\theta_o^{HTR}+(9000-q_h^{HTR})\theta_{ho}^{AHP}}{9000} \tag{21}$$

where, θ_{mix} is the temperature of mixed water, °C; q_h^{HTR} is the water flow further heated by the heater, t/h, considering that the total amount of heating water of the CHP unit is 9000t/h, then the water flow into the header is $9000-q_h^{HTR}$, t/h; θ_o^{HTR} is the outlet water temperature of the heater, °C; θ_{ho}^{AHP} is the outlet temperature of heating water from the AHP, °C.

The power generated by each pressure cylinder are basically same as their internal power. Ignoring the heat loss of each pressure cylinder, the internal power of each pressure cylinder can be calculated according to Eq.(22).

$$N_e^{PC} = D_i^{PC}(h_i^{PC}-h_o^{PC})-\sum_{k=1}^{n}D_o^{PC(k)}(h_o^{PC(k)}-h_o^{PC}) \tag{22}$$

where D_i^{PC} is the inlet steam flow of each pressure cylinder, t/h; h_i^{PC} is the inlet steam enthalpy of each pressure cylinder, kJ/kg; h_o^{PC} is the exhaust steam enthalpy of each pressure cylinder, kJ/kg; $D_o^{PC(k)}$ is the kth extraction steam flow of the pressure cylinder, t/h; $h_o^{PC(k)}$ is the kth extraction steam enthalpy of the pressure cylinder, kJ/kg; n is the number of extraction of each pressure cylinder. All parameters in Eq. (22) can be found in the thermal equilibrium diagram (**TABLE 3**, **TABLE 4** and **TABLE 5**).

Based on the calculation results, the relationship between internal power of each pressure cylinder and their inlet steam flow can be fitted as show in Eq. (23)-(25), and the total power output of the CHP units can be calculated as show in Eq.(26).

$$N_e^{HPC} = 85.245D_i^{HPC}+9318.5 \tag{23}$$

$$N_e^{IPC} = 151.43D_i^{IPC}-7170.1 \tag{24}$$

$$N_e^{LPC} = 191.62D_i^{LPC}-6534.9 \tag{25}$$

$$T_t\frac{dN_e}{dt} = -N_e+(N_e^{HPC}+N_e^{IPC}+N_e^{LPC})\times 10^{-3} \tag{26}$$

where, N_e^{HPC}, N_e^{IPC} and N_e^{LPC} are the internal power of HPC, IPC, and LPC, kW; D_i^{HPC}, D_i^{IPC} and D_i^{LPC} are the inlet steam flow of of HPC, IPC, and LPC, t/h, which can be calculated as $D_i^{HPC}=K_3p_tu_t$, $D_i^{IPC}=100K_7p_r$, $D_i^{LPC}=K_{11}p_o^{IPC}u_i^{LPC}$; N_e is the total power output of the unit, MW; T_t is the inertia time of turbine, and is a unknown parameter that need to be determined.

In summary, the proposed model is as follows:

$$\begin{cases} T_f\dfrac{dq_f}{dt} = -q_f+q_b(t-\tau) \\ C_b\dfrac{dp_b}{dt} = K_1q_f-K_2\sqrt{p_b-p_t} \\ C_t\dfrac{dp_t}{dt} = K_2\sqrt{p_b-p_t}-K_3p_tu_t-K_4p_tu_i^{HPB} \\ C_r\dfrac{dp_r}{dt} = D_r-100K_7p_r-K_8p_ru_i^{LPB} \\ C_h^{HTR}\dfrac{dp_o^{IPC}}{dt} = Q_h^{HTR}-\dfrac{4.1882}{3600} \\ q_h^{HTR}(95.5p_o^{IPC}-\theta_i^{HTR}+93.38) \\ T_t\dfrac{dN_e}{dt} = -N_e+(N_e^{HPC}+N_e^{IPC}+N_e^{LPC})\times 10^{-3} \end{cases} \tag{27}$$

where

$$\begin{aligned} D_r &= K_5K_3p_tu_t+K_6K_4p_tu_i^{HPB}, \\ Q_h^{HTR} &= \frac{1}{3600}D_h^{HTR}(h_o^{IPC}-h_{sw}^{HTR}), \\ D_h^{HTR} &= 100K_9K_7p_r+K_{10}K_8p_ru_i^{LPB}-K_{11}p_o^{IPC}u_i^{LPC} \\ &\quad -K_{12}p_o^{IPC}u_i^{AHP}, \\ \theta_{ho}^{AHP} &= \frac{1.68D_h^{AHP}(h_o^{IPC}-h_{sw}^{HTR})}{q_h^{AHP}c_{px}}+\theta_{hi}^{AHP}, \\ \theta_{mix} &= \frac{q_h^{HTR}\theta_o^{HTR}+(9000-q_h^{HTR})\theta_{ho}^{AHP}}{9000}, \\ R^{HPC} &= \frac{100u_tp_t}{p_r} \\ N_e^{HPC} &= 85.245D_i^{HPC}+9318.5, \\ N_e^{IPC} &= 151.43D_i^{IPC}-7170.1, \\ N_e^{LPC} &= 191.62D_i^{LPC}-6534.9, \quad D_i^{HPC}=K_3p_tu_t, \\ D_i^{IPC} &= 100K_7p_r, \quad D_i^{LPC}=K_{11}p_o^{IPC}u_i^{LPC}, \\ D_h^{AHP} &= K_{12}p_o^{IPC}u_i^{AHP} \end{aligned}$$

The input of model are q_b, u_t, u_i^{HPB}, u_i^{LPC}, u_i^{AHP}, θ_{hi}^{AHP} and q_h^{HTR}; the output of model are p_t, N_e and θ_{mix}; the unknown parameters that need to be determined are $K_1,\ldots,K_{12}$, τ, T_f, C_b, C_t, C_r, C_h^{HTR} and T_t.

2) PARAMETER DETERMINATION

On the basis of the design parameters of the unit (**TABLE 6**), the unknown static parameters K_1 to K_{12} can be calculated as show in Eq.(28) -(40), where the subscript RG represents rated generation condition and RH represents rated heating condition.

$$q_{b(RH)} = q_{b(RG)}\frac{D_{t(RH)}}{D_{t(RG)}} \tag{28}$$

$$K_1 = \frac{D_{t(RH)}}{q_{b(RH)}} \tag{29}$$

$$K_2 = \frac{D_{t(RH)}}{\sqrt{p_{b(RH)} - p_{t(RH)}}} \tag{30}$$

$$K_3 = \frac{D_{t(RH)}}{p_{t(RH)} u_{t(RH)}} = \frac{D_{t(RH)}}{100 p_{1(RH)}} \tag{31}$$

$$K_4 = \frac{D^{HPB}_{i(RH)}}{p_{t(RH)} u^{HPB}_{i(RH)}} \tag{32}$$

$$K_5 = \frac{D_{r(RH)}}{D_{t(RH)}} \tag{33}$$

$$K_6 = \frac{D^{HPB}_{i(RH)} + q^{HPB}_{i(RH)}}{D^{HPB}_{i(RH)}} \tag{34}$$

$$K_7 = \frac{D_{r(RG)}}{100 p_{r(RH)}} \tag{35}$$

$$K_8 = \frac{D^{LPB}_{i(RH)}}{p_{r(RH)} u^{LPB}_{i(RH)}} \tag{36}$$

$$K_9 = \frac{D^{IPC}_{o(RH)}}{D_{r(RG)}} = \frac{D^{IPC}_{i(RH)} + D^{HTR}_{h(RH)}}{D_{r(RG)}} \tag{37}$$

$$K_{10} = \frac{D^{LPB}_{i(RH)} + q^{LPB}_{i(RH)}}{D^{LPB}_{i(RH)}} \tag{38}$$

$$K_{11} = \frac{D^{LPC}_{i(RH)}}{u^{LPC}_{i(RH)} p^{IPC}_{o(RH)}} = \frac{D^{LPC}_{i(RH)}}{100 \frac{p^{LPC}_{i(RH)}}{p^{IPC}_{o(RH)}} p^{IPC}_{o(RH)}} = \frac{D^{LPC}_{i(RH)}}{100 p^{LPC}_{i(RH)}} \tag{39}$$

$$K_{12} = \frac{136.98}{p^{IPC}_o u^{AHP}_i} \tag{40}$$

The dynamic unknown parameters of the model can to be obtained by perturbation test. Considering that the parameter T_f, τ, C_h, T_t of the same type of unit have been studied in [26], this paper directly refers to them, that is $T_f = 120$s, $\tau = 15$s, $C_h = 160$MJ/MPa, $T_t = 12$s. The storage coefficient of drum and main steam pipe are generally determined by perturbation test of main steam valve. During the test, the drum pressure and the main steam flow are recorded, and the total storage coefficient can be calculated as follows:

$$\tilde{C}_b = \frac{\int_0^{t_1} [D_t(t) - D_t(0)]\, dt}{p_b(0) - p_b(t_1)}, \frac{t/h \cdot s}{MPa} \tag{41}$$

The total storage coefficient obtained by the test $\tilde{C}_b = 5308$(t/h·s)/MPa. The storage coefficient of the drum accounts for 90% of the total storage coefficient, while that of main and reheat steam pipe accounts for 10% of the total storage coefficient. Assume that the storage coefficients of the main steam pipe and the reheat steam pipe account for 5% respectively, then the storage coefficient of the drum $C_b = 4777.2$(t/h·s)/MPa, that of main steam pipe $C_t = 265.4$(t/h·s)/MPa, and that of reheat steam pipe $C_r = 265.4$(t/h·s)/MPa. In summary, the model parameters obtained in this paper are shown in TABLE 1.

3) MODEL VERIFICATION

The parameters of the initial conditions are: the coal feed flow is 217.25t/h; the position of main steam valve is 83.16%; the inlet valve position of LPC is 32.4%; the total power output of the unit is 256.29MW; the main steam pressure is 16.7MPa; the exhaust pressure from IPC is 0.49MPa; the extraction steam flow for heating is 500t/h, of which, 397.265t/h of steam enters the heater, 102.735t/h of steam enters the AHP systems; the temperature of return water is 40 °C; the total flow of return water is 9000t/h, 2859.50t/h of the water enters the heater for further heating, 6140.50t/h of water enters the header for mixing.

TABLE 1. Model parameters of the CHP unit.

K_1 =5.7131	K_6 = 1.1914	K_{11} = 14.4375	C_t =265.4
K_2 = 800.1323	K_7 = 2.3257	K_{12} = 5.591	C_r =265.4
K_3 = 0.7512	K_8 = 0.5637	τ = 15	C_h^{HTR} =160
K_4 = 0.1050	K_9 = 0.8447	T_f = 120	T_t = 12
K_5 = 0.8246	K_{10} = 1.1785	C_b =4777.2	

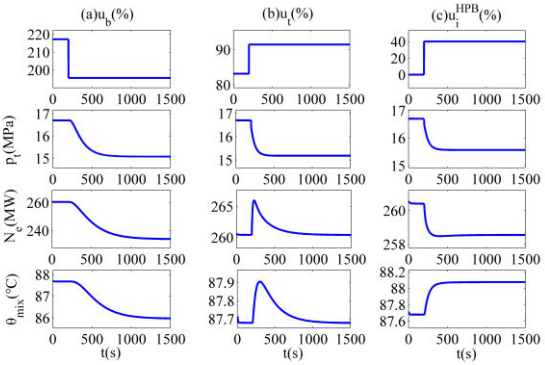

FIGURE 2. Dynamics of the model (I).

FIGURE 2 shows the output of each controlled variable when q_b, u_t and u_i^{HPB} are changed. It can be seen from the figure that: 1) since the response rate of the boiler is slow, there is different degrees of inertia and delay in response of p_t, N_e and θ_{mix} when q_b decreases by 10%, especially for that of θ_{mix}; 2) the p_t drops rapidly and stabilizes at the new state when u_t increases by 10%, the N_e and θ_{mix} return to their initial state after a small overshoot, which is due to the short-time release of the boiler energy storage; 3) since the opening of u_i^{HPB} reduces the amount of steam entering the HPC, the power output of the unit N_e is reduced. The reheat steam pressure is increased simultaneously during the opening of u_i^{HPB}, further increasing the saturation temperature of exhaust steam from IPC, assume that the erminal difference of the heater is constant, then the outlet of water temperature from the heater is increased, eventually leading to an increase in the temperature of the mixed water.

FIGURE 3 shows the output of each controlled variable when u_i^{LPB}, u_i^{LPC} and u_i^{AHP} are changed. It can be seen from the figure that: 1) since the opening of the u_i^{LPB} reduces the amount of steam entering the IPC, the power output of the unit is decreased, but at the same time, the amount of steam

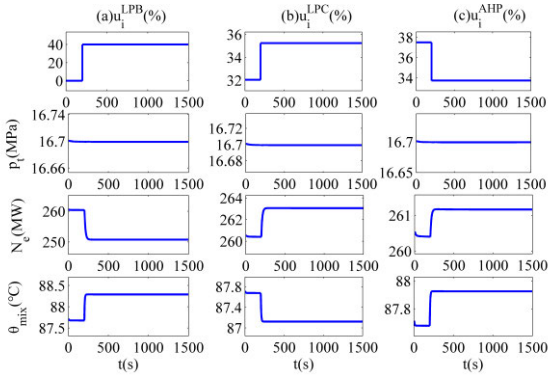

FIGURE 3. Dynamics of the model (II).

entering the heater is increased, thereby increasing the outlet water temperature from the heater; 2) since the opening of the u_i^{LPC} increases the amount of steam entering the LPC, the power output of the unit is increased, but at the same time, the amount of steam entering the heater is decreased, thereby decreasing the outlet water temperature from the heater; 3) since the decrease of u_i^{AHP} increases the exhaust pressure from the IPC, thereby allowing more steam to enter the LPC and the heater, as a result, the power output of the unit and the temperature of the mixed water are increased.

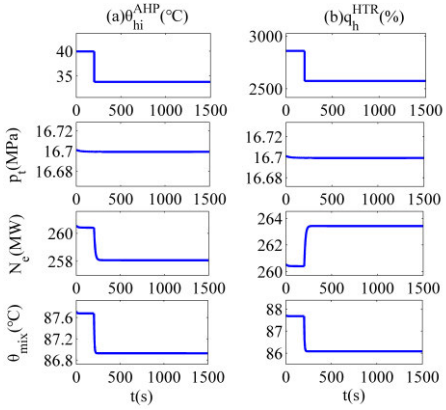

FIGURE 4. Dynamics of the model (III).

FIGURE 4 shows the output of each controlled variable when θ_{hi}^{AHP} and q_h^{HTR} are changed. It can be seen from the figure that: 1) the exhaust pressure from the IPC is decreased when θ_{hi}^{AHP} is decreased, thereby making the amount of steam entering the LPC decrease, as a result, the power output of the unit is decreased; since the heat absorbed from the steam is substantially constant, the decrease of θ_{hi}^{AHP} decreases θ_{mix}; 2) the decrease of q_h^{HTR} decreases the extraction steam pressure from the IPC, thereby making the amount of steam entering the LPC increase C_b, as a result, the power output of the unit is increased; since the heat absorbed from the steam is decreased, the temperature of mixed water is decreased.

FIGURE 5 shows the output of D_i^{HPC}, D_i^{IPC} and R^{HPC} when u_i^{HPB} and u_i^{LPB} are changed. It can be seen from the figure that: 1) the increase of u_i^{HPB} decreases the inlet steam

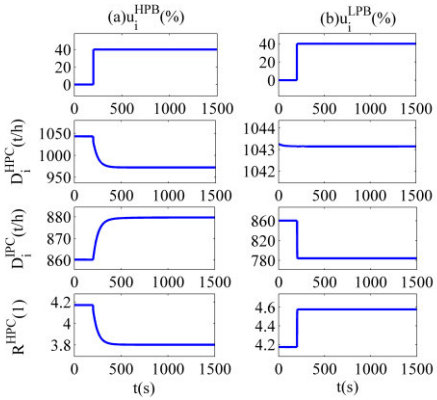

FIGURE 5. Dynamics of the model (IV).

flow of the HPC, but increases the inlet steam flow of the IPC, considering that the axial thrust of cylinders is generally proportional to their steam intake, the balance of the original axial thrust will be broken. Besides, the increase of u_i^{HPB} decreases the R^{HPC}, which will make the exhaust steam pressure and temperature from the HPC increase, in this case, the strength of the final stage blades of the HPC will be weakened. 2) the increase of u_i^{LPB} decreases the inlet steam flow of the IPC, in the same way, the balance of the original axial thrust will also be broken. Besides, the increase of u_i^{LPB} increases the R^{HPC}, which will make the exhaust steam pressure and temperature from the HPC decrease, in this case, the strength of the final stage blades of the HPC will also be weakened. Therefore, it is necessary to coordinate the u_i^{HPB} and u_i^{LPB} to ensure the safe and stable operating of the CHP unit.

C. CONTROL STRATEGY

The design and transformation of the CHP unit's main and auxiliary equipment are the basis for improving its flexibility, and deep peak regulation control is the key. Considering there is large delay and inertia in boiler pulverization and combustion, the traditional PID control algorithm cannot fundamentally solve the control problem of such system. Therefore, this paper takes the predictive control algorithm as the core to design the deep peak regulation control strategy. In order to overcome the effect of known disturbances on the control system, the generalized predictive control algorithm with feedforward-feedback structure is adopted in this paper. The control law is solved in a stair-like manner to avoid the irreversibility of the matrix and ensure the real-time performance of the algorithm. The specific control algorithm and strategy are as follows:

1) PREDICTIVE CONTROL

Consider the following controlled autoregressive integrated moving average model [27], [28]:

$$A\left(q^{-1}\right)y\left(t\right)=B\left(q^{-1}\right)u\left(t-1\right)+C\left(q^{-1}\right)v\left(t-1\right)+\frac{D\left(q^{-1}\right)\xi\left(t\right)}{\Delta} \quad (42)$$

where, $A\left(q^{-1}\right)$, $B\left(q^{-1}\right)$, $C\left(q^{-1}\right)$ and $D\left(q^{-1}\right)$ are n, n_b, n_c and n_d order polynomials of q^{-1}, respectively; $y(t)$ is the output of the system; $u(t)$ is the input of the system; $v(t)$ is the feedforward of the system for decoupling; $\xi(t)$ is the white noise; Δ is the difference operator, $\Delta = 1 - q^{-1}$.

Introducing a Diophantine equation:

$$1 = E_j\left(q^{-1}\right)A\left(q^{-1}\right)\Delta + q^{-j}F_j\left(q^{-1}\right) \tag{43}$$

where, $E_j\left(q^{-1}\right) = e_{j,0} + e_{j,1}q^{-1} + \cdots + e_{j,j-1}q^{-(j-1)}$, $F_j\left(q^{-1}\right) = f_{j,0} + f_{j,1}q^{-1} + \cdots + f_{j,n}q^{-n}$.

After solving the Diophantine equation, the prediction model can be written as:

$$\hat{\boldsymbol{y}} = \boldsymbol{G}\Delta\boldsymbol{u} + \boldsymbol{f} \tag{44}$$

where,

$$\hat{\boldsymbol{y}} = \begin{bmatrix} \hat{y}(t+N_1|t) \\ \vdots \\ \hat{y}(t+N_2|t) \end{bmatrix}, \quad \Delta\mathbf{u} = \begin{bmatrix} \Delta u(\mathrm{t}) \\ \vdots \\ \Delta u(t+N_u-1) \end{bmatrix},$$

$$\boldsymbol{f} = \begin{bmatrix} f_{N_1}(t) \\ \vdots \\ f_{N_2}(t) \end{bmatrix}.$$

Adopt a stair-like manner so that $\Delta u(t) = \delta$, $\Delta u(t+j) = \beta\Delta u(t+j-1) = \beta^j\delta$, then,

$$\begin{aligned}\Delta\boldsymbol{u}(t) &= \left(\Delta u(t), \Delta u(t+1), \cdots, \Delta u(t+N_u-1)\right)^T \\ &= \left(\delta, \beta\delta, \cdots, \beta^{N_u-1}\delta\right)^T = \left(1, \beta, \cdots, \beta^{N_u-1}\right)^T\delta,\end{aligned}$$

and the prediction model in Eq. (44) can be written as:

$$\hat{\boldsymbol{y}} = \tilde{\boldsymbol{G}}\delta + \boldsymbol{f} \tag{45}$$

where, $\tilde{\boldsymbol{G}} = \boldsymbol{G}\left(1, \beta, \cdots, \beta^{N_u-1}\right)^T$.

Assume that the objective function:

$$J = \sum_{j=N_1}^{N_2}\left[w(t+j) - y(t+j)\right]^2 + \lambda\sum_{j=1}^{N_u}\left[\Delta u(t+j-1)\right]^2 \tag{46}$$

where, w is the softening set point of the system; N_1 is the starting value of the prediction horizon; N_2 is the end value of the prediction horizon; N_u is the control horizon; λ is the control weight.

Based on the prediction model in Eq. (45), the objective function can be written as:

$$\begin{aligned}\min_{\delta} J = &\left(\tilde{\boldsymbol{G}}\delta + \boldsymbol{f} - \boldsymbol{w}\right)^T\left(\tilde{\boldsymbol{G}}\delta + \boldsymbol{f} - \boldsymbol{w}\right) \\ &+ \lambda\left(1 + \beta^2 + \cdots + \beta^{2(N_u-1)}\right)\delta^2\end{aligned} \tag{47}$$

Minimize the function $\frac{\partial J}{\partial\delta} = 0$, the control law can be obtained as:

$$\delta = \frac{\tilde{\boldsymbol{G}}^T(\boldsymbol{w} - \boldsymbol{f})}{\tilde{\boldsymbol{G}}^T\tilde{\boldsymbol{G}} + \lambda\left(1 + \beta^2 + \cdots + \beta^{2(N_u-1)}\right)} \tag{48}$$

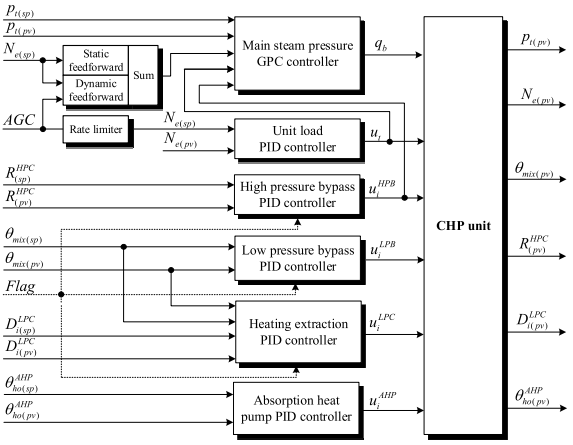

FIGURE 6. Diagram of the deep peak regulation control strategy.

2) STRATEGY DESIGN

Based on the generalized predictive control algorithm, a deep peak regulation control strategy is designed as shown in **FIGURE 6**. This strategy includes a GPC controller for main steam pressure, five PID controllers for unit load, high pressure bypass, low pressure bypass, heating extraction, absorption heat pump respectively, the strategy of each controller is as:

Main steam pressure GPC controller: 1) the static feedforward from $N_{e(sp)}$ is a linear function that converts $N_{e(sp)}$ into coal feed flow roughly, which is used to quantify coal feed flow during load changing process; 2) the dynamic feedforward from AGC and $N_{e(sp)}$ is mainly used to pre-regulate coal feed flow, thus overcoming the problem that the feedback adjustment of the controller is slow in the initial stage of load changing process; 3) the known disturbance feedforward from u_t and u_i^{HPC} is mainly used for the decoupling control of the unit, so as to facilitate the utilization and supplementation of the energy storage timely. The main steam pressure is a signal that can represent the energy balance between the boiler and the turbine, therefore, p_t is selected as the controlled variable.

Unit load PID controller: this controller is generally independent in the DEH system and is mainly used to track the grid load command. Therefore, N_e is selected as the controlled variable.

High pressure bypass PID controller: the exhaust steam pressure from HPB should track the exhaust steam pressure from HPC when the HPB is put into operation, but these two pressures are coupled, the increase of the exhaust steam pressure from HPB will increase the exhaust steam pressure from HPC, in this case, positive feedback control will occur and the safe operation of the turbine cannot be guaranteed. The ratio of the first stage pressure to the exhaust pressure from HPC is a constant during load changing process, if this ratio is kept within a certain range, the safe operation of the turbine can be guaranteed. Therefore, R^{HPC} is selected as the controlled variable.

Low pressure bypass PID controller: the extraction steam flow cannot meet the heat load requirements of residents when the unit is in the deep peaking condition, in this case, the low pressure bypass can be opened to compensate for heating. Therefore, θ_{mix} is selected as the controlled variable. It should be noted that the heat pump can only be put into operation normally if the back pressure of the unit is increased to 7kPa. In this case, the minimum cooling flow of the LPC is 180t/h. Since the cooling flow is the key to ensure the safe operation of the LPC, this paper assumes that the depth peaking signal (Flag) is triggered when $D_{i(pv)}^{LPC} < 200$t/h.

Heating extraction PID controller: the heating capacity of extraction steam can meet the heat load requirements of residents when the unit is in the high load condition, in this case, the steam flow entering the LPC is generally higher than its cooling flow. However, the heating capacity of extraction steam may not meet the heat load requirements of residents when the CHP unit enters the low load condition, in this case, the steam flow entering the LPC may be lower than the cooling flow. Based on the analysis, the heating extraction PID controller actually includes two control loops, one of which controls the heating water temperature (θ_{mix}) in the high load condition, and the other loop controls the steam flow entering the LPC (D_i^{LPC}), so as to ensure the safe and stable operation of the LPC.

Absorption heat pump PID controller: this controller is relatively simple, as long as it operates under the design parameters, its heating efficiency can be guaranteed. Therefore, θ_{hi}^{AHP} is selected as the controlled variable.

3) CONTROL VERIFICATION

During the simulation, the sampling time is 1s, the ramp rate is 6.6MW/min (2% Pe/min). The parameters of the main steam pressure GPC controller are: $N_1 = 70$, $N_2 = 100$, $N_u = 10$, $\lambda = 0.01$, $\alpha = 0.98$, $\beta = 70$; the parameters of the unit load PID controller are: $K_P = 5$, $K_I = 0.01$; the parameters of the high pressure bypass PID controller are: $K_P = 5$, $K_I = 0.4$; the parameters of the low pressure bypass PID controller are: $K_P = 6$, $K_I = 0.2$; the heating extraction PID controller includes two control loops, the parameters of control loop for θ_{mix} are: $K_P = 0.1$, $K_I = 0.05$, the parameters of control loop for D_i^{LPC} are: $K_P = 0.5$, $K_I = 0.01$; the parameters of absorption heat pump PID controllers are: $K_P = 8$, $K_I = 0.04$. The simulation results are shown in **FIGURE 7**, **FIGURE 8**, **FIGURE 9**, **FIGURE 10** and **FIGURE 11**.

FIGURE 7 shows the curve for each controlled variable. It can be seen from the figure that: each controlled variable can closely track its set point, which shows that the control system can adapt to changes in conditions. The mixed water temperature can still be maintained at the design value of 91 °C when the CHP unit enters the low load condition (180MW) (**FIGURE 7 (c)**). Assuming that the minimum load output of the CHP unit without AHP and bypass systems is 230MW, then this deep peak regulation control can free up 50MW of grid space for wind power.

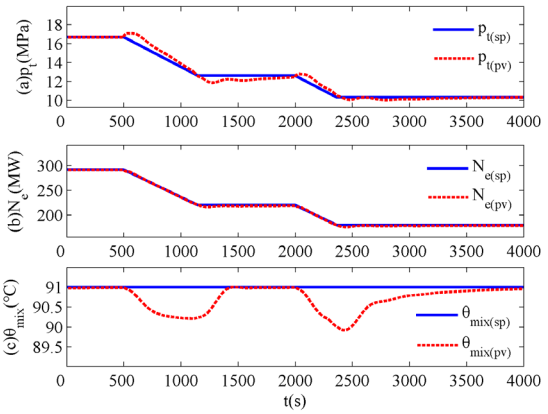

FIGURE 7. Curve for each controlled variable.

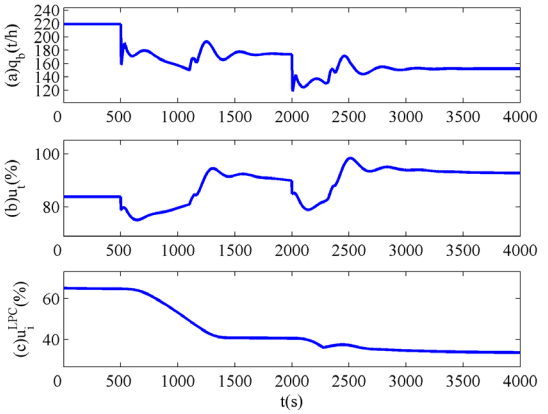

FIGURE 8. Curve for each control variable.

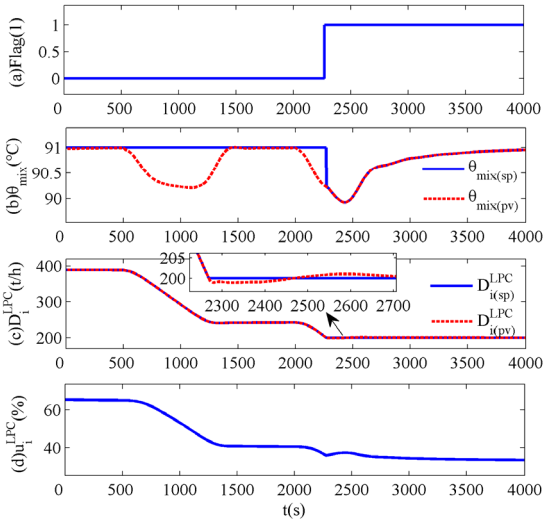

FIGURE 9. Heating extraction controller.

FIGURE 8 shows the curve for each control variable. It can be seen from the figure that the overshoot and fluctuation of coal feed flow are small, the coal feed flow can stabilize at a new state rapidly (**FIGURE 8 (a)**). Since the

TABLE 2. Design parameters of an AHP.

Serial number	Items	Symbol	Unit	Value
1	Heating capacity	$N^{AHP}_{h(RH)}$	MW	53.000
2	heating water flow entering the AHP	$q^{AHP}_{h(RH)}$	t/h	2000.000
3	Inlet temperature of heating water	$\theta^{AHP}_{hi(RH)}$	℃	40.000
4	Outlet temperature of heating water	$\theta^{AHP}_{ho(RH)}$	℃	62.930
5	Circulating water flow entering the AHP	$q^{AHP}_{c(RH)}$	t/h	2333.330
6	Inlet temperature of circulating water	$\theta^{AHP}_{ci(RH)}$	℃	38.000
7	Outlet temperature of circulating water	$\theta^{AHP}_{co(RH)}$	℃	30.000
8	Drive steam pressure	$p^{AHP}_{d(RH)}$	MPa	0.150
9	Drive steam flow	$D^{AHP}_{d(RH)}$	t/h	45.660

TABLE 3. Statistics on parameters of HPC.

Conditions	Inlet steam flow (t/h)	Inlet steam enthalpy (kJ/kg)	Exhaust enthalpy (kJ/kg)	1st extraction flow (t/h)	1st extraction enthalpy (kJ/kg)	2st extraction flow (t/h)	2st extraction enthalpy (kJ/kg)
100%Pe	997.56	3396.9	3040.0	72.6	3157.1	69.92	3040.0
75%Pe	722.00	3432.7	3055.2	45.18	3172.7	44.43	3055.2
50%Pe	483.83	3464.9	3068.9	25.99	3189.4	25.21	3068.9
40%Pe	400.01	3466.3	3073.2	20.27	3196.3	19.22	3073.2
30%Pe	314.66	3464.2	3077.8	14.87	3203.8	13.68	3077.8
Rated extraction	1043.26	3396.9	3050.0	81.20	3173.7	74.34	3050.0
Max extraction	1100.00	3396.9	3060.9	87.99	3187.2	79.65	3060.9

sliding pressure operation mode is adopted in the simulation, the steam flow entering the turbine can decrease naturally with the decrease of main steam pressure, therefore, the main steam valve is maintained at a higher opening degree (**FIGURE 8 (b)**). Since the heating capacity of extraction and AHP can meet the heat load requirements of residents when the unit is in the high load condition, the opening of u_i^{LPC} is reduced during the first load reduction process. However, as the unit load is further reduced, the heating capacity of the extraction and AHP cannot meet the heat load requirements, in other words, the steam flow entering the LPC has been below the cooling flow, in this case, u_i^{LPC} needs to ensure that the steam flow entering the LPC is higher than its cooling flow, therefore, the opening of u_i^{LPC} is not further reduced (**FIGURE 8 (c)**).

FIGURE 9 shows the tracking and bumpless switching of heating extraction controller. The peaking signal (Flag) is triggered when the steam flow entering the LPC is lower than 200t/h (**FIGURE 9(a)**), and then the control loop for θ_{mix} is switched to the control loop for D_i^{LPC} (**FIGURE 9(b)** and **(c)**). The cooling flow can always be kept above 180t/h, therefore, the control system can ensure the safe and stable operation of the LPC (**FIGURE 9(c)**).

FIGURE 10 shows the tracking and bumpless switching of high and low pressure bypass controllers. As the unit load is further reduced, the heating capacity of the extraction and AHP cannot meet the heat load requirements. In this case, the peaking signal Flag is triggered (**FIGURE 10(a)**), the bypass system is put into operation. In the bypass heating

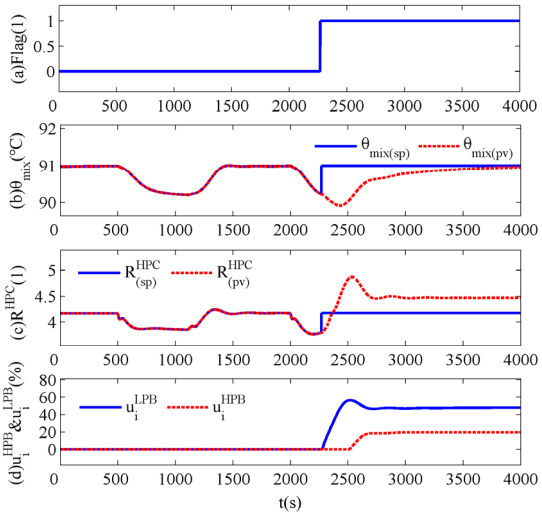

FIGURE 10. High and low pressure bypass controllers.

mode, the low pressure bypass controller is switched to control θ_{mix}, and the high pressure bypass controller is switched to control R^{HPC}. There is a certain range of fluctuations in θ_{mix}, but it can meet the requirement of engineering applications (**FIGURE 10(c)**). Compared with the curve of u_i^{LPB}, that of u_i^{HPB} is smoother and more stable, thereby, the effect of HPB on main steam pressure is weakened.

FIGURE 11 shows the curves of the controlled and control variables of the AHP. It can be seen from the figure that the

TABLE 4. Statistics on parameters of IPC.

Conditions	Inlet steam flow (t/h)	Inlet steam enthalpy (kJ/kg)	Exhaust enthalpy (kJ/kg)	3th extraction flow (t/h)	3st extraction enthalpy (kJ/kg)	4^{th} extraction flow (t/h)		4th extraction enthalpy (kJ/kg)	5th extraction flow (t/h)	5th extraction enthalpy (kJ/kg)
						To deaerator	To turbine			
100%Pe	829.81	3536.1	3020.2	37.9	3331.8	21.68	36.24	3127.2	43.24	3020.2
75%Pe	613.81	3545.3	3029.6	25.12	3340.9	14.85	25.46	3136.6	29.83	3029.6
50%Pe	419.81	3513.5	3009.8	14.72	3314.9	9.19	21.27	3113.9	18.84	3009.8
40%Pe	349.74	3473.7	2983.0	11.36	3281.0	7.33	20.60	3083.9	15.16	2983.0
30%Pe	277.43	3433.8	2955.3	8.04	3247.1	5.46	20.26	3052.8	11.5	2955.3
Rated extraction	860.27	3534.3	2986.0	43.06	3325.6	26.52	38.62	3110.4	30.04	2986.0
Max extraction	903.51	3532.5	2975.4	46.84	3323.0	29.49	41.02	3104.8	29.56	2975.4

TABLE 5. Statistics on parameters of LPC.

Conditions	Inlet steam flow (t/h)	Inlet steam enthalpy (kJ/kg)	Exhaust enthalpy (kJ/kg)	6th extraction flow (t/h)	6th extraction enthalpy (kJ/kg)	7th extraction flow (t/h)	7th extraction enthalpy (kJ/kg)	8th extraction flow (t/h)	8th extraction enthalpy (kJ/kg)
100%Pe	695	3020.2	2313.2	39.13	2817.7	30.78	2628.7	33.48	2478.7
75%Pe	521.68	3029.6	2331.3	27.61	2825.3	21.54	2633.5	19.58	2485.2
50%Pe	357.90	3009.8	2363.3	17.78	2810.3	13.84	2622.6	8.81	2478.9
40%Pe	297.01	2983.0	2378.2	14.39	2789.3	11.24	2607.7	5.43	2466.8
30%Pe	233.49	2955.3	2403.2	11.01	2767.8	8.61	2592.0	2.38	2454.7
Rated extraction	226.67	2986.0	2319.9	11.91	2626.9	9.42	2480.9	2.29	2356.6
Max extraction	211.40	2975.4	2320.4	11.25	2611.9	8.87	2468.4	1.60	2346.1

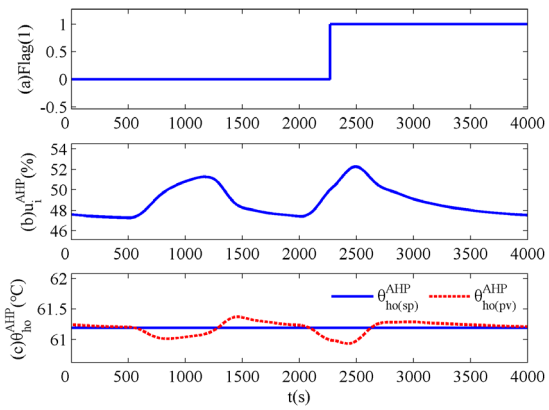

FIGURE 11. Absorption heat pump controller.

outlet temperature of the AHP can track its set point well, especially when the peaking signal Flag is triggered.

III. CONCLUSIONS

The operation mode of CHP units based on "ordering power by heat" is the main reason leading to severe wind power abandonment in northeast China. Decoupling the constraint of "ordering power by heat" for CHP units is an important way to solve this problem. AHP and bypass heating methods are two important ways to decouple this constraint. Firstly, a nonlinear dynamic model of a CHP unit with AHP and bypass systems is proposed to reveal the internal principle of these two methods and their effect on CHP units, in which, the static unknown parameters are determined based on design data, and the dynamic ones are obtained by perturbation test. Simulation results show that the model can reveal the couplings of AHP and bypass system to the CHP unit, and provide model support for controller design. Secondly, a deep peak regulation control strategy is proposed to improve the peaking capacity of the CHP unit, in which, the GPC algorithm with feedforward-feedback structure is adopted to fundamentally solve the control problems of large delay and inertia on the boiler side, and overcome known disturbances on the turbine side; the ratio of the first stage pressure to the exhaust pressure from high pressure cylinder is selected as the controlled variable of high pressure bypass. The deep peak regulation process is divided into two stages: 1) CHP and AHP are used for heating when their heating capacity can meet the heat load requirements of residents, 2) as the unit load is further reduced, bypass mode is activated for heating when the steam flow entering the LPC is lower than its cooling flow. Simulation results show that the control strategy can meet the heat load requirements of residents when the unit is in deep peak regulation condition, the steam flow entering LPC can always be kept above its

TABLE 6. Design parameters of a 330MW CHP unit.

Number	Items	Symbol	Unit	Value
1	Power generation under RG condition	$N_{e(RG)}$	MW	330.000
2	Coal feed flow under RG condition	$q_{b(RG)}$	t/h	207.740
3	Main steam flow under RG condition	$D_{t(RG)}$	t/h	997.560
4	Reheat steam flow under RG condition	$D_{r(RG)}$	t/h	829.810
5	Exhaust steam flow from IPC under RG condition	$D^{IPC}_{o(RG)}$	t/h	695.000
6	Main steam flow under RH condition	$D_{t(RH)}$	t/h	1043.260
7	Reheat steam flow under RH condition	$D_{r(RH)}$	t/h	860.270
8	Exhaust steam flow from IPC under RH condition	$D^{IPC}_{o(RH)}$	t/h	726.670
9	Heating steam flow entering heater under RH condition	$D^{HTR}_{h(RH)}$	t/h	500.000
10	Steam flow entering LPC under RH condition	$D^{LPC}_{i(RH)}$	t/h	226.670
11	Drum pressure under RH condition	$p_{b(RH)}$	MPa	18.590
12	Main steam pressure under RH condition	$p_{t(RH)}$	MPa	16.700
13	First stage pressure under RH condition	$p_{1(RH)}$	MPa	13.887
14	Reheat steam pressure under RH condition	$p_{r(RH)}$	MPa	3.699
15	Exhaust steam pressure from IPC under RH condition	$p^{IPC}_{o(RH)}$	MPa	0.490
16	Inlet steam pressure of LPC under RH condition	$p^{LPC}_{i(RH)}$	MPa	0.157
17	Inlet water temperature of heater under RH condition	$\theta^{HTR}_{i(RH)}$	℃	62.930
18	Steam flow entering HPB under RH condition	$D^{HPB}_{i(RH)}$	t/h	175.000
19	Steam flow entering LPB under RH condition	$D^{LPB}_{i(RH)}$	t/h	208.500
20	Desuperheating water flow entering HPB under RH condition	$q^{HPB}_{i(RH)}$	t/h	33.500
21	Desuperheating water flow entering LPB under RH condition	$q^{LPB}_{i(RH)}$	t/h	37.210

limit value (180t/h), the ratio of the first stage pressure to the exhaust pressure from high pressure cylinder can be always kept within a certain range, therefore, the safe and stable operation of the unit can be guaranteed.

APPENDIX

See Tables 2–6.

REFERENCES

[1] J. Kang, J. Yuan, Z. Hu, and Y. Xu, "Review on wind power development and relevant policies in China during the 11th Five-Year-Plan period," *Renew. Sustain. Energy Rev.*, vol. 16, no. 4, pp. 1907–1915, May 2012, doi: 10.1016/j.rser.2012.01.031.

[2] M. Li, D. Patiño-Echeverri, and J. Zhang, "Policies to promote energy efficiency and air emissions reductions in China's electric power generation sector during the 11th and 12th five-year plan periods: Achievements, remaining challenges, and opportunities," *Energy Policy*, vol. 125, pp. 429–444, Feb. 2019, doi: 10.1016/j.enpol.2018.10.008.

[3] X. Jin, Z. Zhang, X. Shi, and W. Ju, "A review on wind power industry and corresponding insurance market in China: Current status and challenges," *Renew. Sustain. Energy Rev.*, vol. 38, pp. 1069–1082, Oct. 2014, doi: 10.1016/j.rser.2014.07.048.

[4] Z. Yang, Z. Wang, P. Ran, Z. Li, and W. Ni, "Thermodynamic analysis of a hybrid thermal-compressed air energy storage system for the integration of wind power," *Appl. Thermal Eng.*, vol. 66, nos. 1–2, pp. 519–527, May 2014, doi: 10.1016/j.applthermaleng.2014.02.043.

[5] F. Liu, F. Sun, W. Liu, T. Wang, H. Wang, X. Wang, and W. H. Lim, "On wind speed pattern and energy potential in China," *Appl. Energy*, vol. 236, pp. 867–876, Feb. 2019, doi: 10.1016/j.apenergy.2018.12.056.

[6] P. Li, H. Wang, Q. Lv, and W. Li, "Combined heat and power dispatch considering heat storage of both buildings and pipelines in district heating system for wind power integration," *Energies*, vol. 10, no. 7, p. 893, Jun. 2017, doi: 10.3390/en10070893.

[7] S. Rong, Z. Li, and W. Li, "Investigation of the promotion of wind power consumption using the thermal-electric decoupling techniques," *Energies*, vol. 8, no. 8, pp. 8613–8629, Aug. 2015, doi: 10.3390/en8088613.

[8] C. Zhang and Y. Li, "Thermodynamic performance of cycle combined large temperature drop heat exchange process:Theoretical models and advanced process," *Energy*, vol. 150, pp. 1–18, May 2018, doi: 10.1016/j.energy.2018.02.096.

[9] P. A. Østergaard, "Wind power integration in aalborg municipality using compression heat pumps and geothermal absorption heat pumps," *Energy*, vol. 49, pp. 502–508, Jan. 2013, doi: 10.1016/j.energy.2012.11.030.

[10] Y. Gao, Y. Hu, D. Zeng, J. Liu, and F. Chen, "Modeling and control of a combined heat and power unit with two-stage bypass," *Energies*, vol. 11, no. 6, p. 1395, May 2018, doi: 10.3390/en11061395.

[11] L. Yang, X. Zhang, and P. Gao, "Research on heat and electricity coordinated dispatch model for better integration of wind power based on electric boiler with thermal storage," *IET Gener., Transmiss. Distribution*, vol. 12, no. 15, pp. 3736–3743, Aug. 2018, doi: 10.1049/iet-gtd.2017.2032.

[12] M. G. Nielsen, J. M. Morales, M. Zugno, T. E. Pedersen, and H. Madsen, "Economic valuation of heat pumps and electric boilers in the danish energy system," *Appl. Energy*, vol. 167, pp. 189–200, Apr. 2016, doi: 10.1016/j.apenergy.2015.08.115.

[13] X. Liu, J. Wu, N. Jenkins, and A. Bagdanavicius, "Combined analysis of electricity and heat networks," *Appl. Energy*, vol. 162, pp. 1238–1250, Jan. 2016, doi: 10.1016/j.apenergy.2015.01.102.

[14] X. Chen, C. Kang, M. O'Malley, Q. Xia, J. Bai, C. Liu, R. Sun, W. Wang, and H. Li, "Increasing the flexibility of combined heat and power for wind power integration in China: Modeling and implications," *IEEE Trans. Power Syst.*, vol. 30, no. 4, pp. 1848–1857, Jul. 2015, doi: 10.1109/TPWRS.2014.2356723.

[15] S. Katulić, M. Äæehil, and Ž. Bogdan, "A novel method for finding the optimal heat storage tank capacity for a cogeneration power plant," *Appl. Thermal Eng.*, vol. 65, nos. 1–2, pp. 530–538, Apr. 2014, doi: 10.1016/j.applthermaleng.2014.01.051.

[16] M. Zhang and X. Liu, "Flexibility improvement in heating units through low-pressure cylinder excision of 350 MW Heating Unit," *J. North China Electric Power Univ.*, vol. 46, no. 03, pp. 73–79, 2019.

[17] H. Chen, Y. Xiao, G. Xu, J. Xu, X. Yao, and Y. Yang, "Energy-saving mechanism and parametric analysis of the high back-pressure heating process in a 300 MW coal-fired combined heat and power unit," *Appl. Thermal Eng.*, vol. 149, pp. 829–840, Feb. 2019, doi: 10.1016/j.applthermaleng.2018.12.001.

[18] H. S. Zhang, H. B. Zhao, and Z. L. Li, "Performance analysis of the coal-fired power plant with combined heat and power (CHP) based on absorption heat pumps," *J. Energy Inst.*, vol. 89, no. 1, pp. 70–80, Feb. 2016, doi: 10.1016/j.joei.2015.01.009.
[19] W. Li, X. Tian, Y. Li, Y. Ma, and L. Fu, "Combined heating operation optimization of the novel cogeneration system with multi turbine units," *Energy Convers. Manage.*, vol. 171, pp. 518–527, Sep. 2018, doi: 10.1016/j.enconman.2018.06.015.
[20] Y. Li, H. An, W. Li, S. Zhang, X. Jia, and L. Fu, "Thermodynamic, energy consumption and economic analyses of the novel cogeneration heating system based on condensed waste heat recovery," *Energy Convers. Manage.*, vol. 177, pp. 671–681, Dec. 2018, doi: 10.1016/j.enconman.2018.09.091.
[21] Y. Dai, L. Chen, Y. Min, Q. Chen, K. Hu, J. Hao, Y. Zhang, and F. Xu, "Dispatch model of combined heat and power plant considering heat transfer process," *IEEE Trans. Sustain. Energy*, vol. 8, no. 3, pp. 1225–1236, Jul. 2017, doi: 10.1109/TSTE.2017.2671744.
[22] Y. Chen, Q. Guo, H. Sun, Z. Li, Z. Pan, and W. Wu, "A water mass method and its application to integrated heat and electricity dispatch considering thermal inertias," *Energy*, vol. 181, pp. 840–852, Aug. 2019, doi: 10.1016/j.energy.2019.05.190.
[23] H. Demir, M. Mobedi, and S. Ülkü, "A review on adsorption heat pump: Problems and solutions," *Renew. Sustain. Energy Rev.*, vol. 12, no. 9, pp. 2381–2403, Dec. 2008, doi: 10.1016/j.rser.2007.06.005.
[24] D. Zeng, Z. Zhao, Y. Chen, and J. Liu, "A practical 500MW boiler dynamic model analysis," *Proc. CSEE*, vol. 23, no. 5, pp. 149–152, 2003, doi: 10.13334/j.0258-8013.pcsee.2003.05.033.
[25] L. Tian, D. Zeng, J. Liu, and Z. Zhao, "A simplified non-linear dynamic model of 330MW unit," *Proc. CSEE*, vol. 24, no. 8, pp. 180–184, 2004, doi: 10.13334/j.0258-8013.pcsee.2004.08.036.
[26] X. Liu, L. Tian, and Q. Wang, "Simplified nonlinear dynamic model of generating load-throttle pressure-extraction pressure for heating units," *J. Chin. Soc. Power Eng.*, vol. 34, pp. 115–121, Jan. 2014.
[27] D. W. Clarke, C. Mohtadi, and P. S. Tuffs, "Generalized predictive control—Part I. The basic algorithm," *Automatica*, vol. 23, pp. 137–148, Mar. 1987, doi: 10.1016/0005-1098(87)90087-2.
[28] D. W. Clarke, C. Mohtadi, and P. S. Tuffs, "Generalized predictive control—Part II extensions and interpretations," *Automatica*, vol. 23, no. 2, pp. 149–160, Mar. 1987, doi: /10.1016/0005-1098(87)90088-4.

YAOKUI GAO received the Ph.D. degree in electrical engineering from North China Electric Power University, China, in 2019. He joined North China Electric Power University, in 2019, where he is currently holding a postdoctoral position in electrical engineering. He has made great achievements in this field, especially in the field of coordinated control systems. His research interest includes modeling and optimal control of complex thermal systems in thermal power plants.

DELIANG ZENG received the Ph.D. degree in electrical engineering from North China Electric Power University, China, in 2000. He is currently the Director of the Beijing Key Laboratory of New Technology and System of Industrial Process Measurement and Control, North China Electric Power University, where he is also the Full-Time Researcher with the State Key Laboratory of Alternate Electrical Power System with Renewable Energy Sources. He mainly studies the modeling and control of thermal process and intelligent optimization control of complex systems.

LIXIA ZHANG received the B.S. degree in automation from North China Electric Power University, Beijing, China, in 2018, where she is currently pursuing the M.S. degree in control theory and control engineering. She mainly studies the soft sensing model of key parameters of thermal power unit-based on principle analysis and data identification, where she has made great achievements in this field.

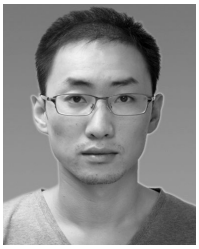

YONG HU received the Ph.D. degree in control theory and control engineering from North China Electric Power University, Beijing, China, in 2015. He is currently holding a postdoctoral position in energy engineering with the Mechanical Engineering College, North China Electric Power University. He has been engaged in the research of intelligent power generation operation control systems and modeling and optimal control of thermal power plant for a long time.

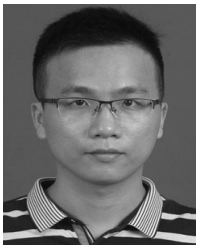

ZEKUN XIE is currently pursuing the Ph.D. degree in control theory and control engineering with North China Electric Power University, Beijing, China. He is mainly interested in condition detection and diagnosis of thermal system equipment, where he has made great achievements in this field.